Operating an In-Cabin Femto-Cellular System Within a Given LTE Cellular Network

Tezcan Cogalan, *Student Member, IEEE*, Stefan Videv, and Harald Haas, *Fellow, IEEE*

***Abstract*—An onboard mobile communication system can be operated when the height of an aircraft is above 3000 m and the maximum equivalent isotropic radiated power outside an aircraft is below −13 dBm for 200 kHz bandwidth in a 1800 MHz system based on the Electronic Communications Committee reports. However, in order to provide seamless connectivity for aircraft passengers, the onboard communication system should be in operation in every phase of the flight. Therefore, in this paper, the compatibility of an in-cabin long term evolution (LTE) 1800 MHz femto cellular system with the current terrestrial LTE 1800 systems are investigated when an aircraft is stationary on the ground. Edinburgh Airport in Scotland and the existing LTE cells that provide network coverage at the airport are modeled through a simulation platform. Three Airbus A321 aircraft are modeled, while stationary, in the parked position on the apron and an in-cabin LTE femto cellular system is deployed within each aircraft. Signal-to-noise-plus-interference ratio and power leakage from the in-cabin evolved NodeBs in the downlink direction are considered as performance metrics to investigate the coexistence of the terrestrial and in-cabin systems. The simulation results show that the in-cabin LTE 1800 MHz femto cellular system can be operated without causing any significant interference to the existing terrestrial LTE 1800 MHz system while the aircraft is parked on the apron. However, it may be advisable to only operate the system when the aircraft doors are closed, in order to mitigate any possible interference effect on the users who are boarding the aircraft through the passenger boarding bridge. According to the results shown for a linear apron concept, the legislation governing the onboard mobile communication systems should be revised, in order to pave the way to the goal of seamless mobile connectivity in the next generation of communication systems.**

***Index Terms*—.**

I. Introduction

In THE early years of the telecommunication industry, mobile services were limited to text and voice transmissions. Service providers supplied these services by deploying cells with a range of up to 20 km in rural areas and up to 1 km in urban areas. For these services, time division multiple access (TDMA) which uses operated frequency band for a user on a time basis, was used to serve multiple users. When the number of mobile subscriptions increased and data transmission took place among the already available text and voice services, service providers had to shrink their deployed cells in order to improve their service quality in terms of connectivity and throughput. Also, code division multiple access (CDMA) technique which spreads the user signal across the entire bandwidth at a time and uses a code for each user, was used in order to serve multiple users at a time. However, mobile subscriptions and the demand for higher mobile data rates were increasing. Due to the used access technology, interference became a system limiting factor with an increased number of cells. Therefore, an enhanced access scheme was needed in order to deploy more, smaller cells.

Nowadays, the telecommunication industry is in its fourth generation (4G) and discussions on fifth generation (5G) technologies are ongoing. 4G is also known as Long Term Evolution (LTE) and designed to provide a smooth transition to 5G. LTE systems use orthogonal frequency division multiple access (OFDMA) scheme in downlink and single carrier frequency division multiple access (SCFDMA) scheme in uplink directions. The orthogonality feature of both of the schemes provide efficient use of the operated frequency band and mitigate the interference among evolved nodeB (eNB) as well as user equipment (UE). Therefore, deploying smaller cells, named femtocells, is possible in LTE systems by mitigating interference. Moreover, along with enhancements of wireless technology, LTE system can establish a cooperation among cells with coordinated multipoint transmission (CoMP), sense environment with cognitive radio (CR), aggregate operated frequency bands with carrier aggregation (CA) and centrally adapt its control decisions with software defined network (SDN) and network function virtualization (NFV) technologies.

As noted, LTE is the path to 5G and the key feature of 5G is accessing data anywhere and anytime for anyone and anything. Although seamless mobility is the key requirement of 5G, having a mobile connection for aircraft passengers has recently gained the attention of industry and academia. The reason behind the postponement of onboard mobile connectivity was due to the prohibition of using mobile devices within the aircraft. In 1963, the first regulation on using mobile devices onboard an aircraft was published by the Federal Aviation Administration (FAA). Although it is commonly believed that mobile devices are prohibited due to security issues, in actuality, the regulation is based on the fact that the onboard mobile devices have a potential to interfere with aircraft radios, as well as terrestrial wireless

Manuscript received September 25, 2017; revised March 13, 2018 and April 24, 2018; accepted April 27, 2018. Date of publication May 16, 2018; date of current version August 13, 2018. The authors acknowledge financial support by Airbus GmbH, Hamburg, Germany. Professor Harald Haas acknowledges support by the UK Engineering and Physical Sciences Research Council (EPSRC) under Grant EP/K008757/1. The review of this paper was coordinated by Dr. X. Dong. *(Corresponding author: Tezcan Cogalan.)*

The authors are with the School of Engineering, Institute for Digital Communications, Li-Fi R&D Centre, The University of Edinburgh, Edinburgh EH9 3FD, U.K. (e-mail: t.cogalan@ed.ac.uk; s.videv@ed.ac.uk; h.haas@ed.ac.uk).

Color versions of one or more of the figures in this paper are available online at http://ieeexplore.ieee.org.

Digital Object Identifier 10.1109/TVT.2018.2837345

network [1]. In 1991, the Federal Communications Commission (FCC) released its rules to ban the airborne use of mobile devices [2]. At that time, TDMA was used as the access technology, and as noted, once a user is assigned for transmission, it uses the whole operated frequency band. Also, adaptive power allocation was not used at that time. Therefore, concerns about the interference caused by using mobile devices onboard an aircraft to terrestrial network were reasonable.

However, today it is possible, as a result of the noted technological enhancements, to deploy one or more small cells inside an aircraft. Also, it is possible to adaptively allocate transmission power per UE. Due to the decreased distance between transmitter and receiver in small cells, it is possible to provide a sufficient quality of service to small cell users with low transmission powers. As a matter of fact, minimizing the potential of interference from aircraft mobile users to terrestrial users is possible. Accordingly, revising the prohibition on mobile connectivity for aboard aircraft passengers is considered by the FCC [2], [3] and the Electronic Communications Committee (ECC) [4]–[8].

Deployment and compatibility of mobile communication services on board aircraft and ground-based systems have been studied for Global System for Mobile Communications (GSM) and Universal Mobile Telecommunications System (UMTS) in [4]–[6]; and for LTE in [7], [8]. In ECC reports, the onboard communication system is analysed for the GSM 1800 MHz, UMTS 2100 MHz and LTE 1800 MHz and 2600 MHz systems. In [7], due to the radar services in the band adjacent to 2600 MHz, LTE 2600 MHz system is found to be incompatible and it is not considered for the onboard communication systems. Therefore, 1800 MHz frequency band is considered for the onboard LTE systems. Based on the ECC reports and decisions, the in-cabin mobile system should only be operated when the altitude of the aircraft is 3000 m or more, and the system should not be operated while the aircraft is on the ground or during take-off and landing [4]. According to [7], [8], when the altitude of the aircraft is 3000 m, the maximum equivalent isotropic radiated power (EIRP) from in-cabin eNB to outside the aircraft must not exceed -13 dBm for 200 kHz (or 1 dBm for 5 MHz) of a 1800 MHz LTE system (frequencies between 1805 and 1880 MHz) to prevent service degradation at the ground-based systems. This limit corresponds to a maximum increase of the received noise floor of 1 dB. However, this limit is independent of the characteristics of the aircraft, such as size and fuselage attenuation; and proposed communication system such as number of eNBs, type of antennas, signal propagation and output power of the eNB [4]. Additionally, it is suggested that in order to prevent in-cabin UE sets trying to access the terrestrial LTE network, a network control unit (NCU) should be operated. The NCU is used to raise the noise floor inside the cabin. Therefore, the quality of the signal received from the in-cabin eNBs will become higher than the terrestrial eNBs and, the in-cabin UE sets will not attempt to access the terrestrial network. The same goal can be achieved through radio frequency (RF) shielding of the aircraft. The RF shielding of the aircraft increases the signal attenuation of the aircraft fuselage. Thus, the quality of the signal received from the terrestrial eNBs will be much lower than the signal received from the in-cabin eNBs. Therefore, the in-cabin UE sets will try to access the in-cabin network, not the terrestrial network.

TABLE I
DIMENSIONS OF AIRCRAFT

Number of Rows	35	Aisle width	50 cm
Number of Seats	205	Row width	80 cm
Seat width	60 cm	Cabin width	395 cm
Seat height	110 cm	Cabin height	249 cm

In order to provide truly seamless and user-friendly integration of an onboard communication system, it is important that the users can make use of the system as soon as they step on board the aircraft. Therefore, an onboard communication system should be in operation in all phases of a flight, from taxi out and take-off to landing and taxi in. In this study, the effects due to the operation of the in-cabin LTE femto cellular system on the existing terrestrial LTE network are investigated, when an aircraft is on the ground at its parking position. Particular focus of this study is dedicated to determine the downlink interference power due to the in-cabin LTE eNBs that terrestrial users experience, as well as the effects of the terrestrial systems on the operation of the in-cabin deployment. Accordingly, Edinburgh Airport and LTE cells which cover Edinburgh Airport are modeled to investigate overall downlink interference with and without the operation of the in-cabin LTE system. How to provide a backhaul link to the aircraft is out of the scope of this study. Interested readers can refer to [9], [10], where providing the backhaul link to an aircraft is studied in detail by means of economical and technical perspectives.

The rest of the paper is structured as follows. Sections II and III introduce the considered in-cabin and terrestrial LTE system models, respectively. The overall system assumptions are given in Section IV. Section V describes the performance metrics considered in this study. The simulation framework is presented in Section VI and its performance results are given in Section VII. Conclusions and recommendations are given in Section VIII.

II. IN-CABIN LTE FEMTO CELLULAR SYSTEM

A. Aircraft In-Cabin

A medium-sized aircraft is around 30–38 m long and has a capacity of 150–250 passengers. In order to provide high data rate to each passenger, more than one cell deployment is needed for such a user dense environment. Therefore, a multi-cell LTE 1800 MHz deployment inside an Airbus A321 aircraft is considered. The Airbus A321 aircraft cabin is a medium-sized commercial aircraft configured with 35 rows of seats and a single aisle. Seating capacity of the Airbus A321 aircraft is 205 passengers. The approximated cabin interior dimensions are given in Table I.

In this study, in-cabin LTE eNBs are deployed as in [11]. According to [11], each aircraft has 2 eNBs which are operated within LTE band 3 (1800 MHz -3×20 MHz channels and 1×15 MHz channel). In the deployment, each eNB is equipped with 2×1 directional patch antennas and a sectorization is employed with 40° antenna tilt. According to the employed sectorization, each eNB has two channels pointed towards the cockpit of the aircraft and two channels pointed towards the tail

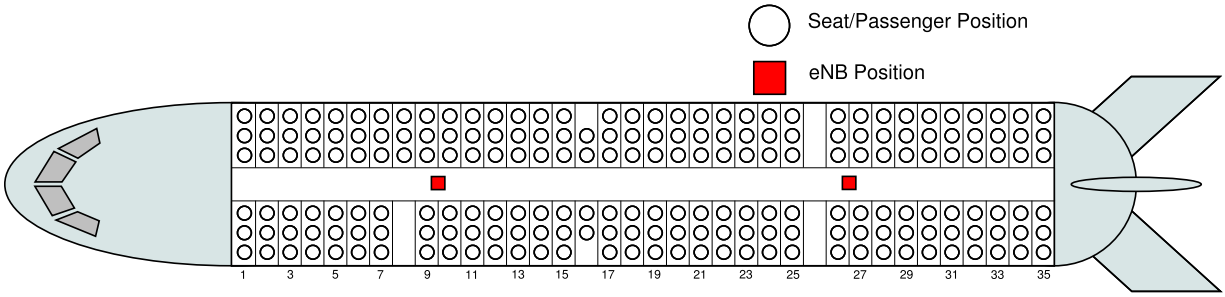

Fig. 1. Cabin layout of Airbus A321.

of the aircraft[1]. Fig. 1 shows considered Airbus A321 aircraft cabin layout and deployed eNB positions.

B. In-Cabin Channel Model

A log-distance path loss model for in-cabin channel propagation was obtained in [12] based on an in-cabin channel measurement campaign conducted in a medium-sized commercial aircraft. However, the given path loss model in [12] was constructed for fixed antenna parameters. As noted, in order to improve the quality of service for aircraft in-cabin users, multiple eNBs are deployed with tilted directional antennas. Therefore, in the path loss calculation, the used antenna characteristics should be considered. In [11], the path loss model given in [12] is modified to consider antenna characteristics. In this study, the overall signal attenuation given in [11] for 1800 MHz is used to obtain channel between in-cabin eNBs and aircraft passengers. Accordingly, the overall signal attenuation $\mathrm{PL_{AC}}$ is calculated as:

$$\mathrm{PL_{AC}[dB]} = \mathrm{PL_{in\text{-}cabin}}(d) - G_{T_x} - G_{R_x} - G_{\mathrm{pattern},T_x}, \quad (1)$$

where $\mathrm{PL_{in\text{-}cabin}}$ is the in-cabin path loss model given in [12]; G_{T_x} and G_{R_x} are the transmitter and receiver antenna gain, respectively; and G_{pattern,T_x} is the transmit antenna pattern gain[2].

Once the overall signal attenuation between the in-cabin eNBs and aircraft passengers is obtained, the channel response of each resource block (RB) is generated by:

$$H^{\mathrm{AC}}_{\mathrm{RB}}(f_{\mathrm{RB}}) = \sqrt{10^{\frac{-\mathrm{PL_{AC}}}{10}}}\, H^{\mathrm{AC}}(f_{\mathrm{RB}}), \quad (2)$$

where $H^{\mathrm{AC}}_{\mathrm{RB}}(f_{\mathrm{RB}})$ is the channel frequency response of the RB; and $H^{\mathrm{AC}}(f_{\mathrm{RB}})$ is a Rician distributed frequency-selective fading term of the RB due to multipath environment. The frequency-selective fading terms are obtained based on the measurement results given in [12]. The details of the used parameters in the in-cabin path loss model can be found in [12].

III. Terrestrial LTE System

A. Edinburgh Airport

Edinburgh Airport is located in Ingliston, a town 5 miles west of the City Center. The airport is one of the busiest in the UK, with an average of 33,880 passengers and over 333 flights per day [14]. The airport is comprised of two runways and one terminal, with one domestic and two international arrival halls. There are a total of 23 aircraft gates which are structured based on the linear apron concept described in [15]. The map of Edinburgh Airport was obtained from the Google maps service as shown in Fig. 2.

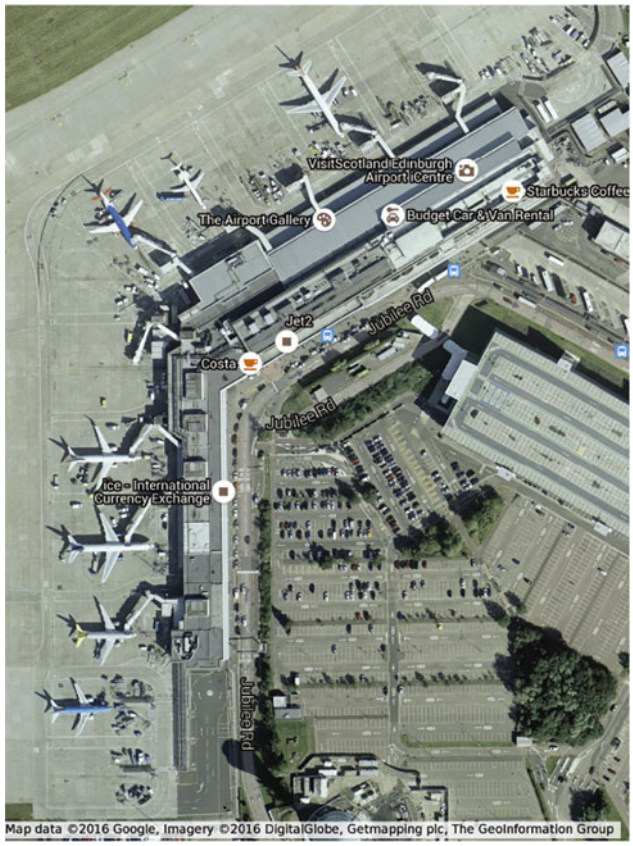

Fig. 2. Overview of Edinburgh Airport.

B. Existing LTE eNBs

In the UK, there are four main wireless cellular network operators: EE, O2, H3G and Vodafone [16]. Each operator uses different frequencies to deliver mobile services. The permitted frequency bands used in the UK for LTE are: 800 MHz, 1800 MHz and 2600 MHz. The LTE frequency bands used by the mobile network operators are shown in Table II [16]. As the frequency band of the in-cabin LTE system uses the band of 1800 MHz between 1805 and 1880 MHz for downlink, the downlink interference from operators of H3G and EE is investigated. The interference from the in-cabin LTE femto cellular

[1]For illustrations of sectorization, please see Figs. 1 and 2 in [11].
[2]G_{pattern,T_x} is obtained according to the equations given in [13].

TABLE II
CELLULAR OPERATORS IN THE UK AND THEIR LICENSED LTE FREQUENCY BANDS

Operator	Frequency		
	800 MHz	1800 MHz	2600 MHz
EE	2×5 MHz	2×45 MHz Downlink: 1831.7 - 1876.7 MHz Uplink: 1736.7 - 1781.7 MHz	2×35 MHz
H3G	2×5 MHz	2×15 MHz Downlink: 1816.7 - 1831.7 MHz Uplink: 1721.7 - 1736.7 MHz	-
O2	2×10 MHz	-	-
Vodafone	2×10 MHz	-	2×20 MHz 1×25 MHz

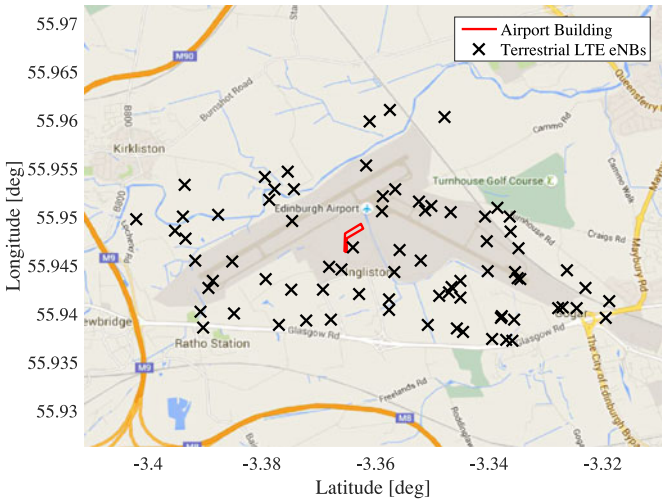

Fig. 3. Edinburgh Airport and existing LTE eNBs on Google Map.

system to terrestrial LTE users around and inside Edinburgh Airport is also investigated.

Accordingly, geographical coordinates of the existing LTE eNBs of the operators EE and H3G around Edinburgh Airport are obtained from OpenSignal website. An overall map of Edinburgh Airport with LTE eNBs that serve the airport area is shown in Fig. 3.

C. Terrestrial Channel Model

As part of the WINNER II [17] and WINNER+ [18] projects, path loss models of different scenarios have been investigated. These models are based on literature and real measurements taken during the WINNER II and WINNER+ projects. The general form of the logarithmic path loss model can be expressed as:

$$\mathrm{PL} = A \log_{10}(d) + B + C \log_{10} \frac{f_c}{5} + X, \tag{3}$$

where A is the path loss exponent; d is the distance between base station (BS) and mobile station (MS); B is the intercept which is determined by the free space path loss for the reference distance; C is the frequency dependent path loss; f_c is the carrier frequency; and X is the environment dependent term. Specifically, the logarithmic path loss model is modified according to different environments, such as line of sight (LoS) or non-line of sight (NLoS) links, suburban or urban environments, and indoor or outdoor scenarios. The considered WINNER scenarios in this study are listed below [17]:

- **B1 Urban Microcell Scenario (UMi):** The height of the eNB and UE antennas is assumed to be well below the tops of surrounding buildings.
- **B4 Outdoor-to-Indoor Scenario (O2Ia):** In an outdoor to indoor urban microcell scenario. It is assumed that the UE antenna height is at 1-2 m (plus the floor height), and eNB antenna height below roof-top, at 5-15 m depending on the height of surrounding buildings. The variation of eNB antenna height depends on surrounding buildings, basically over the height of four floors.
- **C1 Suburban Macrocell Scenario (SMa):** Macro eNBs are located well above the roof tops to allow wide area coverage and UE handsets are outdoors at street level. Buildings are typically low residential detached houses (1-2 floors) or flats with few floors.
- **C2 Urban Macrocell Scenario (UMa):** UE is located at outdoors at street level and fixed eNB clearly above surrounding building height. Non- or obstructed LoS is a common case.
- **C4 Urban Macro Outdoor-to-Indoor Scenario (O2Ib):** Outdoor environment is the same as in C2, and the indoor environment is an office environment. The eNB antenna is clearly above the average building height. Long LoS channels to indoor environment walls is a common case.

The path loss models for the considered scenarios can be found in [17], [18]. There are different outdoor path loss models for LoS and NLoS cases, respectively. The NLoS case provides a shadowing standard deviation higher than that for LoS. Due to the blocking effect of walls and ceilings, there is a severe shadowing fading in the outdoor-to-indoor case. For example, the shadowing standard deviation is $\sigma = 7$ for scenario B4 and $\sigma = 10$ for scenario C4 [17].

Therefore, if an eNB is an urban microcell, and the distance between UE and eNB is relatively short, scenario B1 with LoS is appropriate. Otherwise, there is a high probability of NLoS case. The LoS link probability of scenario B1, $P_{\mathrm{B1,LOS}}$ can be written as:

$$P_{\mathrm{B1,LOS}} = \min(18/d, 1)(1 - \exp(-d/36)) + \exp(-d/36), \tag{4}$$

where $\min(x, y)$ is the function to take the minimum between x and y. Also, if the UE is indoors, such as in an airport gateway or inside the aircraft, the outdoor-to-indoor scenario B4 is used. If the eNB is a suburban macrocell, scenario C1 is applied and the LoS probability is:

$$P_{\mathrm{C1,LOS}} = \exp(-d/200). \tag{5}$$

If the eNB is an urban macrocell, scenario C2 should be used and the LoS probability is:

$$P_{\mathrm{C2,LOS}} = \min(18/d, 1)(1 - \exp(-d/63)) + \exp(-d/63). \tag{6}$$

Once the distance dependent path loss is calculated, a clustered delay line (CDL) model specific to each scenario is used to generate frequency selective fading coefficients. The CDL models based on cluster and power delay profile values for each scenario can be found in [17]. According to the CDL model,

time-domain channel response is calculated as follow:

$$h'(t) = \sum_i \sqrt{a_i} h_{w_i} \delta(t - \tau_i), \tag{7}$$

where a_i is the power delay value of the ith cluster of the applicable CDL model; h_{w_i} is a random variable with zero mean and unity variance; and τ_i is the delay of the ith cluster of the applicable CDL model. When the time-domain channel response $h'(t)$ is calculated, the frequency-domain response of the channel can be found by its Fourier transform as:

$$H_0(f) = \sum_i \sqrt{a_i} h_{w_i} e^{-j2\pi f \tau_i}, \tag{8}$$

where $H_0(f)$ is the frequency-domain fast fading channel information for the frequency f. Thus, in order to calculate channel response of each RB, the frequency band of the channel should be appropriately quantized.

Accordingly, the final channel impulse response, including the shadowing, can be calculated as:

$$H_{\mathrm{RB}}(f_{\mathrm{RB}}) = \sqrt{10^{\frac{-\mathrm{PL} + X_{\sigma_{\mathrm{SF}}}}{10}}} H_0(f_{\mathrm{RB}}), \tag{9}$$

where $H_{\mathrm{RB}}(f_{\mathrm{RB}})$ is the channel frequency response of RB; PL is the distance dependent path loss based on the considered scenario; $X_{\sigma_{\mathrm{SF}}}$ is the log-normal shadowing value based on the considered scenario; and $H_0(f_{\mathrm{RB}})$ is the channel frequency response of center frequency of the RB.

IV. System Model

A. Frequency Reuse

LTE uses frequency reuse 1, which means all available RBs are used by every eNB. In general, the terrestrial eNBs are sectorized in three sectors and uses full frequency reuse. As noted, sectorization is also used for the in-cabin eNBs to increase the effective distance of the interfering source. For the in-cabin eNBs, full frequency reuse is applied where the 4 available channels (3×20 MHz and 1×15 MHz) are divided into two sectors, and each two are pointed in opposite directions.

B. User-eNB Attachment

In the considered system model, each in-cabin user is connected to an eNB which serves the best average signal power to the user. However, for the terrestrial users, two different user-eNB association schemes are considered. The first scheme is the same approach used to attach in-cabin users, each terrestrial user is served by the eNB that provides the best average signal power. In the second scheme, a terrestrial user can associate to the eNB that serves the best average signal power as long as there is room for the user at the eNB. In other words, there is a limitation on the number of attached users to an eNB in the second scheme. This can be considered as load balancing in the network. Accordingly, the first scheme can be considered as the best case scenario where a user always has the best possible desired signal power, and the second scheme can be considered as the real-world scenario where there is no guarantee to serve a user from the eNB which could best serve the user.

C. Scheduling

In order to investigate changes in the interference level with and without an in-cabin LTE system, scheduling is out of scope for this study. Accordingly, it is assumed that all available RBs in each eNB/channel are always being transmitted on for each user. In other words, it is assumed that each user is served by all available RBs at its connected eNB.

V. System Performance Analysis

In light of the given system model assumptions, to investigate the effects of the in-cabin LTE system to the already existing terrestrial LTE network as well as effects of the existing terrestrial LTE network to the in-cabin LTE system when the aircraft is in parking position, four different cases are considered as follows:

- **CASE 1: Only terrestrial LTE system:** In this case, the in-cabin LTE system is not considered in operation, and only the terrestrial LTE system performance is investigated to consider it as a benchmark for terrestrial users.
- **CASE 2: Full-scale LTE system:** In addition to the existing terrestrial LTE network, in-cabin LTE system with 2 eNBs deployed in the aircraft on the airport apron is considered. This case can also be considered as the overall network model where all of the eNBs are considered as in operation.
- **CASE 3: Only in-cabin LTE systems:** To investigate how the nearby in-cabin LTE deployments interact between each other, only the in-cabin LTE systems are considered. In this case, all the terrestrial eNBs are out of operation and all the in-cabin eNBs are in operation.
- **CASE 4: Only single in-cabin LTE system:** Isolated in-cabin LTE system is considered to use as a benchmark while investigating the in-cabin user performance affected by the terrestrial LTE network, as well as the other nearby in-cabin deployments. Different from the case 3, in this case, a single in-cabin LTE system deployed in an aircraft is considered as in operation. All the remaining eNBs are considered as out of operation.

A. Interference Analysis

For the described cases, received signal strength indicator (RSSI) is considered as a performance metric. The reason for considering RSSI as a performance metric is twofold: (i) interference power level can be obtained by comparing different system cases that described above; and (ii) RSSI measurement results can be found in any mobile device which is connected to a mobile network. Therefore, interference analysis given in this report can be verified by a simple mobile device (with no need to do measurements with an expensive software).

Based on third generation partnership project (3GPP) definitions, RSSI represents the wideband received power which includes the power from serving cell, non-serving (interfering) cells and noise, observed in certain orthogonal frequency division multiplexing (OFDM) symbols [19]. Therefore, comparing RSSI performance of different cases gives information on changes in the received power level between the cases. For example, obtaining the received power level difference between

the system with (case 2) and without (case 1) in-cabin eNBs gives an information on how much interference is caused by in-cabin eNBs.

In LTE systems, a RB consists of 7 OFDM symbols, each OFDM symbol has 12 subcarriers and each subcarrier has 15 kHz spacing [20]. Thus, a RB consists of 84 subcarriers and corresponds to 180 kHz in the frequency domain. Among the OFDM symbols, only 2 of them (first and fifth OFDM symbols) carry the reference signal. RSSI is obtained by averaging the received power of 12 subcarriers located in each OFDM symbol that carries the reference signal.

Obtaining RSSI of a user is dependent on used RBs at the connected cell and the cells using the same RBs in the given case. Let x be the case index, $\mathcal{C}$ be the set of all cells considered in the system, c be the cell index and r be the used RB index at the cell c that serves the user u. Firstly, obtain the set $\mathcal{C}_x$ which represents the active cells in the case x. For example, in case 1, all the terrestrial cells will be considered whereas, in case 2 the terrestrial and in-cabin cells will be considered. Then, obtain the set $\mathcal{C}_x^r$ which represents the cells that use the RB r. Accordingly, it can be written that $\mathcal{C}_x^r \subseteq \mathcal{C}_x \subseteq \mathcal{C}$. Therefore, RSSI of a user for case x, $P_{u,x}^{\text{RSSI}}$ is obtained by:

$$P_{u,x}^{\text{RSSI}} = \left(\frac{1}{7}\right)\left(\sum_{c\in\mathcal{C}_x^r}\sum_{r=1}^{N_{\text{RB},c}} P_{u,c,r}\right), \tag{10}$$

where $P_{u,c,r}$ is the received power on RB r from cell c to user u; and $N_{\text{RB},c}$ is the total number of RBs used in cell c. The factor of $1/7$ used in (10) is to calculate RSSI based on 3GPP definitions where as noted, 2 out of 7 OFDM symbols use reference signals in a RB and the received power on subcarriers in these symbols are averaged. In this study, channel gain is obtained based on a RB level. In order to obtain the average received power level of the 2 OFDM symbols, the received power of a RB should be divided by the number of symbols in a RB, which is equal to 7. The parameter $P_{u,c,r}$ is calculated based on the transmission power and number of RBs used in cell c as well as channel coefficients between the cell c and user u on RB r as:

$$P_{u,c,r} = \left(\frac{\sqrt{P_c}}{N_{\text{RB},c}} H_r^{u,c}\right)^2, \tag{11}$$

where P_c is the transmission power at cell c; and $H_r^{u,c}$ represents channel coefficients. $H_r^{u,c}$ is obtained by (2) or (9) when cell c is an in-cabin LTE cell or terrestrial LTE cell, respectively.

B. SINR Analysis

As noted, RSSI gives information on the average total received power. It can only be affected by the number of deployed eNBs, their transmission power and inherently, channel coefficients between the mobile device and eNBs. When there is a limitation on the number of attached users per eNB, a user may not attach to its best serving eNB and forced to connect to its second best eNB. The RSSI level of this user will be the same. Therefore, the effect of having a limitation on the number of attached users cannot be observed from the RSSI level. However, in such a situation, the signal-to-noise-plus-interference ratio (SINR) which is the ratio between the desired signal and undesired signals including noise, performance of the user will be degraded. Therefore, SINR performance is considered in order to investigate interaction between the in-cabin and terrestrial LTE systems when there is a constraint on number of users per eNB. SINR of a user u on RB r for a case x, $\gamma_{u,r,x}$, is calculated as:

$$\gamma_{u,r,x} = \frac{P_{u,c^*,r}}{\sum\limits_{\substack{c\in\mathcal{C}_x^r \\ c\neq c^*}} P_{u,c,r} + N_r}, \tag{12}$$

where c^* is the cell that user u is connected to; and N_r is the noise power. The noise power N_r is computed by utilizing the well known thermal noise power equation $N_r = kTB_r$, where k is Boltzmann's constant; T is the temperature in Kelvin; and B_r is the bandwidth of a RB, which is 180 kHz as noted.

C. Handover Analysis

In order to provide a user-friendly integration of an in-cabin communication system, it is important that the users can make use of the system as soon as they step on board the aircraft. In communication systems, when a neighbouring cell provides better signal quality than the connected cell, the user will connect to the neighbouring cell. This process is called cell re-selection when a user is in idle-mode[3] and called as handover when a user is in connected mode[4]. In LTE, these processes are triggered by eNB based on measurement reports sent by UE. Therefore, cell re-selection and handover are a UE assisted, eNB triggered processes in LTE.

When the UE is attached to one of the cells, it becomes a part of the network and periodically measures reference signal received power (RSRP) and reference signal received quality (RSRQ) levels based on the reference signal (RS) received from the connected and neighbour cells, which are the cells adjacent to the connected cell. Before the UE conducts any measurement, the eNB specifies the type of measurement, which is called an "event" in LTE. Based on the measurement reports sent by UE, the eNB decides to trigger cell re-selection or the handover process. Triggering these processes can be based on the RSRP level, RSRQ level or both. The triggering quantity depends on the eNB configuration and is sent to UE via system information block (SIB) messages. When the trigger quantity is achieved by a neighbouring cell, the serving eNB decides whether to handover the UE or not.

In Fig. 4, the measurement event A3, which is the case where the neighbour cell becomes offset better than the connected cell, is depicted. As shown in Fig. 4, RSRP is chosen as the trigger quantity and there are offset and hysteresis parameters added to the serving cell RSRP. The offset parameter is used to make the serving cell attractive in order to decrease the number of handovers. The hysteresis parameter is used to discard small fluctuations and make sure that the UE has a stronger signal from a neighbouring cell. On the other hand, there is another offset value used for the neighbouring cell, called *cellIndividualOffset*.

[3]When the user has no dedicated resources for transmission, this is called idle mode and means that the UE just transmits and receives control messages.

[4]When the user is in the connected mode, it transmits and receives data messages.

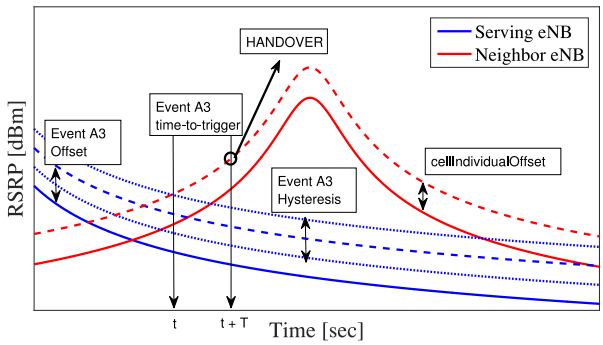

Fig. 4. Handover in event A3.

This parameter is used to extend the range of a cell, termed cell range extension (CRE) in LTE. CRE method is used in heterogeneous networks to force a user, which is connected to a highly loaded macrocell, to connect a lightly loaded small (pico or femto) cell. Therefore, the *cellIndividualOffset* parameter artificially increases the received signal quality of a cell in order to offload the highly loaded cells.

As shown in Fig. 4, when the artificial RSRP of the neighbouring cell exceeds the triggering threshold of the serving cell, event A3 is triggered. At this point, the handover process has not happened yet. The event A3 is triggered with a *time-to-trigger* parameter. The *time-to-trigger* is a duration that UE performs frequent measurements of the signal quality of the serving and neighbouring cells. The purpose of using such a time interval before handover the UE is to avoid a ping-pong effect[5]. Therefore, when the *time-to-trigger* duration is finished and filtered[6] signal quality measurement of the neighbouring cell is better than the serving cell, then the eNB decides to handover the UE to the cell which provides better signal quality. Accordingly, the parameters *a3-Offset*, *hysteresis*, *cellIndividualOffset* and *time-to-trigger* are needed to be known to make the transition from the terrestrial to in-cabin system smoothly.

VI. Simulation Model

A. Physical Model

In the simulation platform, Edinburgh Airport, including the airport building, gates and apron, is physically modeled based on its coordinates. In addition, the existing LTE eNBs of each operator are modeled. The height of each eNB is randomly assigned as 10 m or 25 m. Then, three Airbus A321 aircraft are modeled as parked on the airport apron where each of them has a connection to the airport building by a passenger boarding bridge (referred to as the gateway in this study).

Once all the physical buildings and cells are modeled, in-cabin and terrestrial users are modeled. As shown in Fig. 1, all passenger seats represent a user. Terrestrial users are considered as 3 different classes – airport indoor users, gateway users who are waiting to board the aircraft and aircraft ground service users. In total, 4 different classes of user are considered, including in-cabin users alongside the aforementioned ones. The location of the airport indoor users and ground service users are randomly distributed inside the airport and around each aircraft, respectively. However, the gateway users are uniformly distributed to model them as if they are waiting in a line within the gateway. The geometrical model of Edinburgh Airport, existing LTE eNBs, in-cabin eNBs and users are shown in Fig. 5.

B. Path Loss and Channel Model

As noted in Sections II-B and III-C, the model given in [11] and WINNER+ channel models are used to model the channel from in-cabin eNBs to terrestrial users as well as terrestrial eNBs to all users, both the in-cabin and terrestrial users. Accordingly, when a link from an in-cabin eNB to a terrestrial user is considered, indoor-to-outdoor scenario B4 is used to model path loss. Also, when a link from a terrestrial eNB to an in-cabin user is considered, the same scenario B4 is used to model outdoor-to-indoor link path loss. For both cases, the aircraft fuselage attenuation which will be explained in more detail in the next section, is added to the calculated path loss. However, when a link from a terrestrial eNB to a terrestrial users is considered, WINNER scenario and link case (LoS or NLoS) decision is made as follows:

- Step 1 - Check the height of the eNB,
  - if it is 10 m, the eNB is microcell and the scenario should be B1 or B4;
  - if it is 25 m, the eNB is macrocell and the scenario should be C1, C2 or C4.
- Step 2 - Check the link from the eNB to the user,
  - if the number of wall intersection points is larger than 1, the link is definitely NLoS;
  - otherwise, the link can be LoS or NLoS based on its distance dependent LoS probability which is given in (4),(5) and (6) for scenarios B1, C1 and C2, respectively.

In Fig. 6, the calculation of the number of wall intersection points is depicted. When the channel between the user and eNB A is considered, there is only one intersection point on the path of the signal propagation, which means that between eNB A and the airport building wall, the channel could be a LoS one. However, when the channel between a user and eNB B is considered, there are 3 intersection points along the line of signal propagation. Accordingly, the link from eNB B to the airport building wall is definitely NLoS. The same approach can be used to characterize the channel between the eNBs inside the 1st and 3rd aircraft where the 2nd aircraft is in parking position between the other two. Thus, all the channels from/to eNBs inside the 1st aircraft as well as to/from the 3rd aircraft are definitely NLoS channels.

C. Aircraft Fuselage Attenuation

Based on ECC reports [5], [7], three different aircraft fuselage attenuation cases, namely case A, case B and case C, are considered. The aircraft fuselage attenuation level is assumed as 5 dB, 10 dB and 15 dB for case A, case B and case C, respectively. In this study, the described aircraft fuselage attenuation cases A and C are considered. Accordingly, as noted, the channel

[5]A ping-pong effect is the term used to describe a situation that a UE is continuously handedover between the same two cells.

[6]In LTE, UE applies a filtering (averaging) for all measurements (except for UE transmitter-receiver time difference, RSSI and channel occupancy measurements) before evaluating or reporting the measurement result.

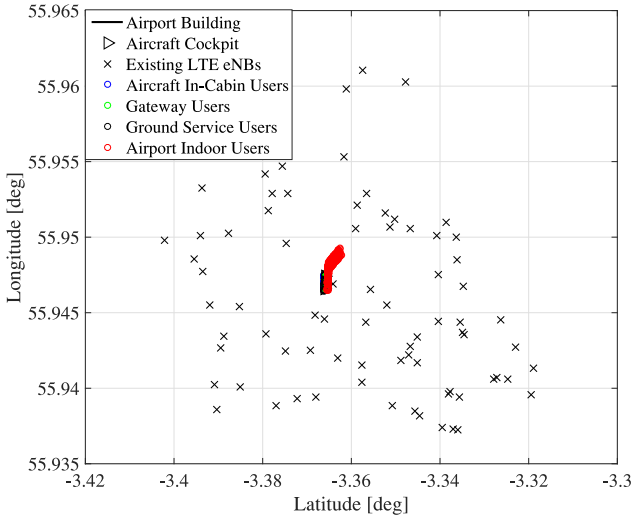

(a) Full-scale

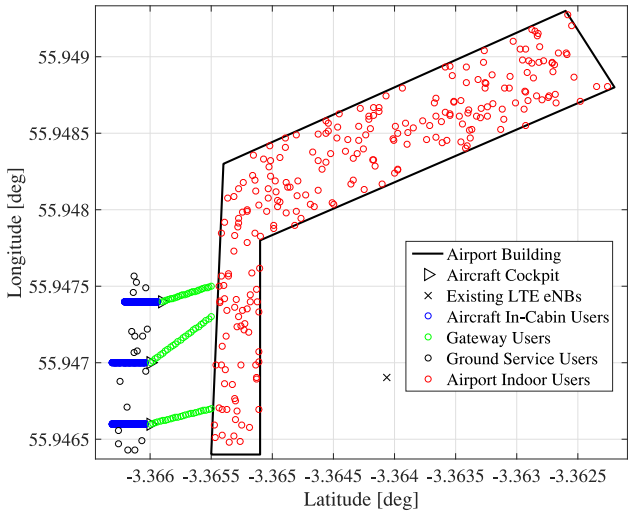

(b) Zoomed

Fig. 5. Simulation model. (a) Full-scale. (b) Zoomed.

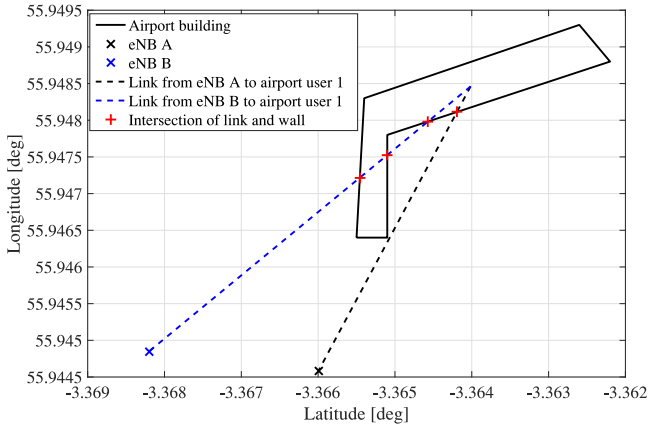

Fig. 6. LoS and NLoS channels.

from/to in-cabin eNBs/users are attenuated an additional 5 dB or 15 dB to model the aircraft fuselage for cases A or C, respectively. When channels between the aircraft are considered, the attenuation is added twice as expected in order to model from aircraft-to-air and from air-to-aircraft transmissions.

D. Transmission Power and Antenna Gain

Based on [7], [13], antenna input power is assumed as 43 dBm for 5 MHz channel, and 46 dBm for 10 Hz, 15 MHz and 20 MHz channels in downlink of the LTE 1800 MHz system. However, in [21], the maximum permitted downlink transmission power for LTE 1800 MHz is increased by 3 dB for operators in the UK which covers operators EE and H3G. Accordingly, the antenna input power is assumed as 46 dBm for 5 MHz channel and 49 dBm for 10 MHz, 15 MHz and 20 MHz channels in downlink of the system. Also, maximum allowable EIRP is stated as 65 dBm [21] which is the summation of the antenna input power and antenna gain. In the simulations, antenna gain of the terrestrial eNBs is set to 15 dBi [13] and assumed as uniform in each direction to simulate an omni-directional antenna. Although the terrestrial eNBs are generally deployed as in three sectors with directional antennas, assuming uniform gain in each direction makes the system as the worst case scenario.

For the in-cabin LTE 1800 MHz system, the antenna input power is assumed as 10.2 dBm due to the short distance between eNBs and users inside the aircraft. The antenna gain of the used 2×1 directional patch antennas is 12 dBi. Accordingly, for the in-cabin eNBs, an EIRP of 22.2 dBm is considered.

E. Simulation Parameters

The system parameters used within the simulation adhere to the LTE specifications and operator licenses. A list of all the parameters is summarized in Table III.

VII. Simulation Results

Performance of the in-cabin LTE system within the existing LTE network is simulated and the results are given below. The system performance evaluation is based on 500 Monte Carlo simulations, where in each simulation the terrestrial users are randomly located. As noted in Section V, RSSI and SINR are considered as the performance metrics for four different cases. Accordingly, RSSI and SINR performance of the terrestrial users are observed when the in-cabin LTE eNBs are not in operation, which is the case 1. RSSI and SINR performance are also observed for the in-cabin users when there is no transmission from the terrestrial and nearby in-cabin LTE eNBs, which is the case 4. As noted in Section V, the case 1 and case 4 are the benchmark for the terrestrial and in-cabin users, respectively. In addition to the performance observation for the cases 1 and 4, RSSI is observed for the case 3, by considering the only in-cabin LTE eNBs in operation. After that, full-scale LTE system (case 2) is considered by operating all, the in-cabin and terrestrial, eNBs. Then, in order to understand the interaction among the terrestrial and in-cabin LTE systems, the benchmark cases are compared with the full-scale system case.

TABLE III
SIMULATION PARAMETERS

In-Cabin LTE System Parameter	Value
Total bandwidth	75 MHz
RB bandwidth	180 kHz
Total number of RBs	375
Subcarriers per RB	12
time slot (TS) duration	0.5 ms
OFDM symbols per TS	7
Total number of channels	4
Channel 1 frequency band	1805-1825 MHz (1×20 MHz; 100 RBs)
Channel 2 frequency band	1825-1845 MHz (1×20 MHz; 100 RBs)
Channel 3 frequency band	1845-1860 MHz (1×15 MHz; 75 RBs)
Channel 4 frequency band	1860-1880 MHz (1×20 MHz; 100 RBs)
Antenna input power	10.2 dBm
Tx antenna gain	12 dBi
Rx antenna gain	0 dBi
Tx antenna height (from cabin floor)	1.8 m
Rx antenna height (from cabin floor)	1.1 m
Tx antenna type	2×1 Directional Patch
Tx antenna tilt	40^o
Total number of eNBs	2
Total number of users	205
Aircraft fuselage attenuation	5 dB, 15 dB
Frequency reuse	1
Terrestrial LTE System Parameter	**Value**
Operator H3G frequency band	1816.7-1831.7 MHz (1×5 MHz + 1×10 MHz; 75 RBs)
Operator EE frequency band	1831.7-1876.7 MHz (3×15 MHz; 225 RBs)
Antenna input power - 5 MHz	46 dBm
Antenna input power - 10, 15, 20 MHz	49 dBm
Tx antenna gain	15 dBi
Rx antenna gain	0 dBi
Tx antenna height (from ground)	10 or 25 m
Rx antenna height (from ground/floor)	1.5 m
Tx antenna type	Omni-directional
Tx antenna tilt	0^o
Total number of EE eNBs	50
Total number of H3G eNBs	26
Total number of gateway users	50 per aircraft
Total number of ground service users	8 per aircraft
Total number of airport indoor users	250
Frequency Reuse	1
Terrestrial LTE System Parameter	**Value**
Boltzmann's constant	1.38×10^{-23} Joule/Kelvin
Temperature	5500 Kelvin

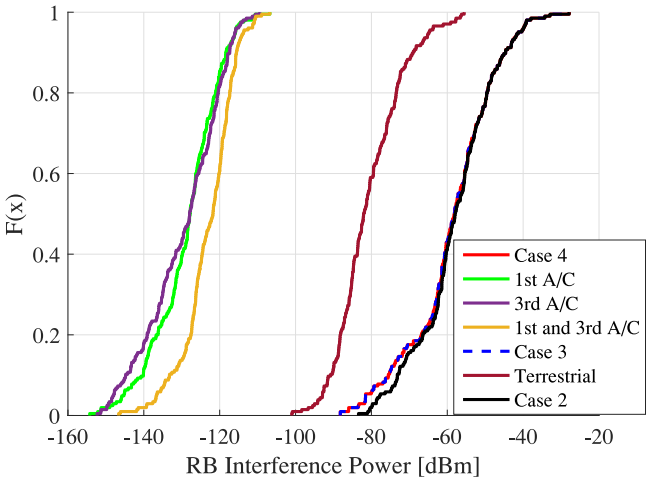

Fig. 7. Received interference power levels for in-cabin users inside the second aircraft. "A/C" stands for aircraft.

In the performance result figures, the function $F(X)$ refers to the cumulative distribution function (CDF) which is defined as the probability of the random variable X takes on values less than or equal to x.

A. Interference Power Results

In order to evaluate the transmission power leakage from the aircraft to the outside, as well as from the outside to the aircraft, eNBs inside the second aircraft, which is parked between the other two aircraft, are considered. In Fig. 7, the received interference power level of users inside the second aircraft are shown for different numbers of aircraft and described

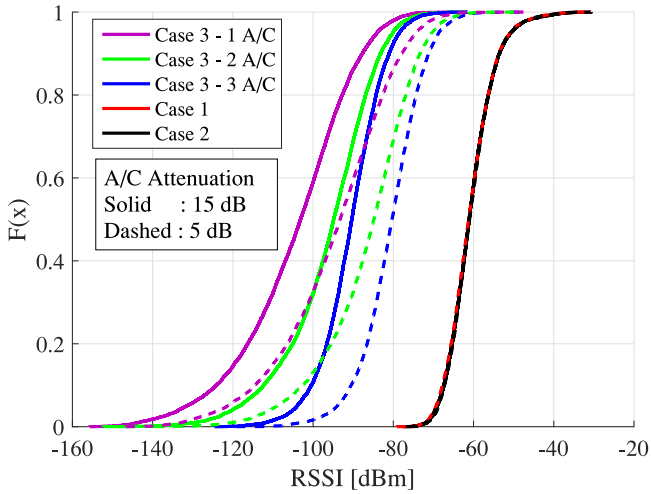

Fig. 8. Received interference power levels outside the second aircraft. "A/C" stands for aircraft.

simulation cases 2, 3 and 4. It can be clearly seen from Fig. 7 that the interference signal from one aircraft to another has almost no effect on the given linear apron concept[7]. This is due to the aircraft fuselage attenuation, which is considered as 5 dB, the distance between the aircraft and the transmission power used in the in-cabin eNBs. As noted, in the proposed in-cabin LTE system, eNB antennas are pointed to the cockpit and tail of the aircraft by using directional antennas. Thus, signal propagation is constrained on the pointed direction and the side lobe propagation is minimized. Moreover, the interference power from the terrestrial eNBs to the users inside the aircraft has slightly increased the received interference power for 20% of the in-cabin users. However, it is important to note that the main interference source of the in-cabin users is the other eNB deployed inside the same aircraft. The received interference power level within the same onboard system inside the second aircraft is around 70 dB and 20 dB higher than the received power level from the other two aircraft and terrestrial eNBs, respectively. Therefore, it can be said that based on the position of the aircraft parking spots, where the minimum distance between the spots are fixed for all airport aprons, and the given onboard system deployment, increasing the number of aircraft does not increase the interference power level among the onboard systems.

In order to investigate the transmission power leakage from in-cabin eNBs to the outside of the aircraft, received power level from the in-cabin eNBs at outside the aircraft is obtained inside a circle with a radius of 50 m around the second aircraft[8]. In Fig. 8, the received interference power level of different number of aircraft and fuselage attenuation levels are shown. When the number of aircraft parked on the apron is increased, the median of the received interference power level increases. However, the

[7]Although the distance between the nose of two aircraft may shorter than the aircraft wing span for a concept where several aircraft facing each other, there will be an additional wall attenuation due to the airport terminal building inbetween the facing aircraft. Therefore, for other airport apron concepts, it is unlikely that interference will be higher than the linear concept where several aircraft are parked side by side.

[8]Based on the given system model, the second aircraft is located 44 m away from the both first and third aircraft.

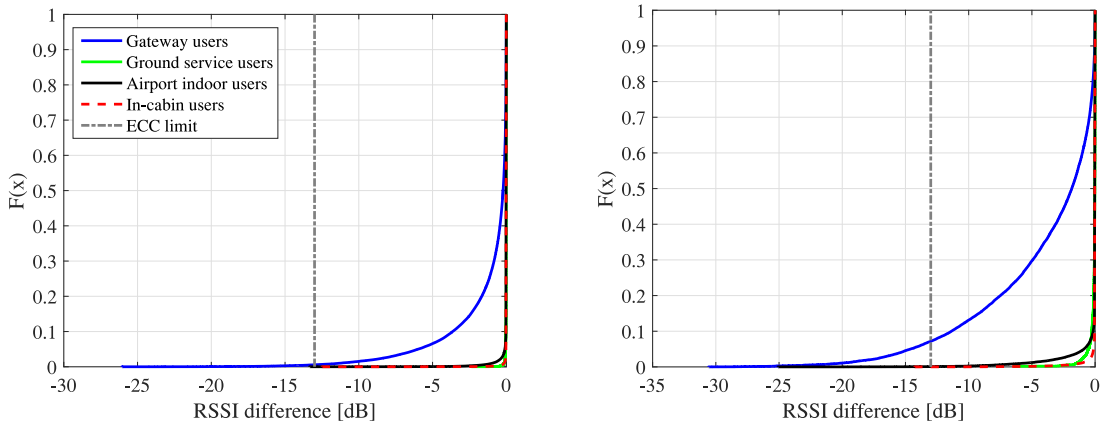

(a) 15 dB fuselage attenuation (b) 5 dB fuselage attenuation

Fig. 9. RSSI difference between the systems with and without in-cabin LTE system. (a) 15 dB fuselage attenuation. (b) 5 dB fuselage attenuation.

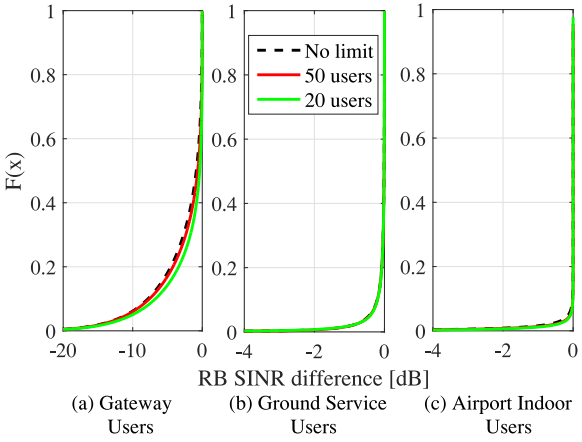

(a) Gateway Users (b) Ground Service Users (c) Airport Indoor Users

Fig. 10. Effect of number of users limit per eNB.

maximum value of the interference is not changed. This is due to the architectural plan used in airport aprons. The minimum distance between the aircraft parking spots depends on regulations to standardized it independent from the type and size of an aircraft. When the power leakage from the 1st and 3rd aircraft is considered for the users on the ground around the 2nd aircraft, it will only affect the users close to these aircraft. Therefore, the median of the received interference power CDF is increased but the maximum received level remains the same. The same observation can be made for both aircraft fuselage attenuation levels. Inherently, for a low attenuation level, the power leakage increases but increasing the number of aircraft in the system does not change the maximum received interference level. Moreover, when the interference power level from all 3 aircraft is taken into account for the users around the 2nd aircraft, there is no change on the overall received interference power level independent from the considered fuselage attenuation. This is due to having relatively higher interference from other terrestrial eNBs than the in-cabin eNBs in the system.

The RSSI performance of the users in the considered system is investigated as well. Fig. 9 shows the CDF of the experienced RSSI difference between the systems with and without in-cabin LTE eNBs. When the performance of the in-cabin users is considered, a notable RSSI degradation is not observed. Therefore, as noted, it can be understood that the terrestrial LTE eNBs do not contribute to the interference level inside the aircraft in the downlink direction. However, the in-cabin LTE eNBs cause interference to the gateway users. This could potentially result in the connectivity in an area close to the aircraft doors being compromised. Although the in-cabin eNB causes an increase in the interference power level, exceeding the limit considered by the ECC is only observed for 0.005% and 0.07% of the gateway users when the aircraft fuselage attenuation is considered as 15 dB and 5 dB, respectively. It is clear that due to the aircraft fuselage attenuation, the used in-cabin transmission power, the airport wall attenuation and distance between the apron and the airport, the least vulnerable users are the ones inside the airport. Based on the simulation results, for 15 dB fuselage attenuation, the RSSI performance of airport indoor users is essentially the same as when the in-cabin LTE system is transmitting and when it is not. This is the case for the ground service users as well. There is no significant additional interference power caused by the in-cabin LTE eNBs. Although the RSSI performance of airport indoor and ground service users are slightly increased for the 5 dB fuselage attenuation, it is still far below the ECC's limit.

B. SINR Results

As noted, SINR performance is observed in order to investigate the effects of having limitation on the number of users that an terrestrial eNB can serve. 20 users per eNB, 50 users per eNB and unlimited users per eNB cases are simulated and compared. As described in Section IV-B, the given user number is the maximum capability limit for a terrestrial eNB. It is important to note, the given user capability limitation is only applied to the terrestrial eNBs, not to the in-cabin eNBs. When an terrestrial eNB has reached its maximum capability number, it will not accept the connection request from a user. The declined user has to connect to another terrestrial eNB, which is not its best serving eNB. Therefore, when the systems with and without limitations on the number of users that an eNB can serve are compared, a SINR performance degradation is expected. However, as noted, the focus of this study is to understand how the in-cabin eNBs interact with the terrestrial network. From this perspective, when a terrestrial user cannot connect to its best

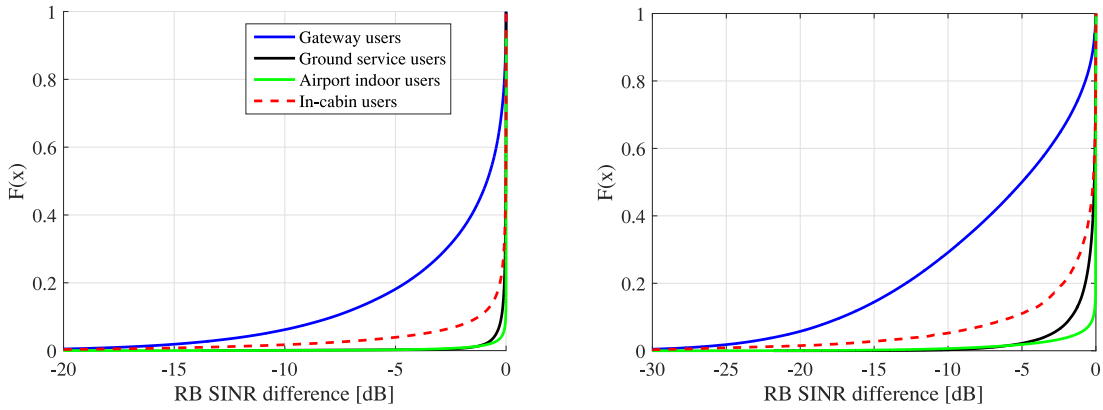

(a) 15 dB fuselage attenuation (b) 5 dB fuselage attenuation

Fig. 11. SINR difference per RB between the systems with and without in-cabin LTE system. (a) 15 dB fuselage attenuation. (d) 5 dB fuselage attenuation.

serving eNB and is forced to connect to another terrestrial eNB, its main interference source will become its best serving eNB. Therefore, it is expected that the SINR performance degradation due to interference generated by the in-cabin eNBs in operation is negligible.

Fig. 10 shows the observed SINR difference between the systems with and without in-cabin eNBs for different class of users when there is a limitation on the number of users per eNB. According to the Fig. 10, having a number of users per eNB limitation has a negligible effect on the RB SINR performance. When three cases for the number of users per eNB are considered for the gateway users, the SINR performance degradation due to the existence of in-cabin eNBs is getting lower with decreasing the number of users per eNB, as expected. Although a small degradation in the SINR performance can be seen for the gateway users, the considered three cases for the number of users that an eNB can serve have exactly the same SINR performance per RB for the ground service and airport indoor users. The capacity of RBs appears to be minimally affected by the given eNB user capability limits.

In Fig. 11, the SINR difference per RB is shown for the eNBs with unlimited user capability in order to make a fair comparison between the performance of the terrestrial and in-cabin users. When the observed RSSI difference performance given in Fig. 9 is taken into account, it is expected that the SINR difference observed for the in-cabin, ground service and airport indoor users should be the same. However, as shown in Fig. 11, the SINR difference of the in-cabin users is slightly larger than the SINR difference performance of the ground service and airport indoor users, irrespective of the considered fuselage attenuation. This can be explained by the considered EIRP for the in-cabin LTE system which is 22.2 dBm and relatively lower than the EIRP values considered for the terrestrial LTE system.

In general, activating the in-cabin LTE system does not have a significant harmful effect on the existing terrestrial LTE network and its users. Especially since, realistically, there are limitations on the number of users that an eNB can serve, contribution of the in-cabin eNBs to the interference level is negligible. The main interference source becomes the terrestrial eNBs. Although, the performance of several RBs is decreased, the majority of the RBs have the same performance with and without the in-cabin system being operational.

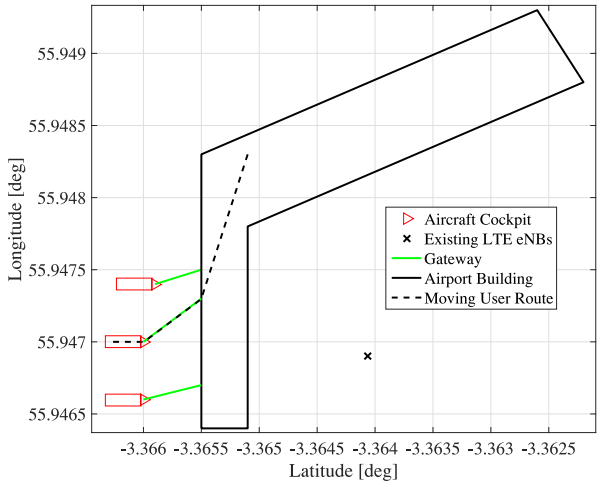

Fig. 12. Moving user route.

C. Handover Results

In order to analyse the handover triggering for a passenger boarding the aircraft, a moving user is modeled in the system where it starts its move from inside the airport, then travels through the gateway to board the aircraft and walks to end of the cabin. The speed of the moving user is assumed to be 3 km/h (0.82 m/s) and its path is shown in Fig. 12.

Fig. 13 shows handover instances along the moving user path. Handover triggering quantity is considered as RSRP. The range of the handover parameters are given in Table IV. The parameters *a3-Offset*, *hysteresis* and *time-to-trigger* are set to 12 dB, 6 dB and 1024 ms, respectively. The *individualCellOffset* is considered as 0 dB for terrestrial eNBs and 3 dB for in-cabin eNBs. As it is shown in Fig. 13(b), as the moving user steps onto the aircraft, it is handed over to the in-cabin eNB.

For the considered system model, the received signal power level varied from eNB to eNB. However, in order to understand all perspectives of the compatibility of the terrestrial and

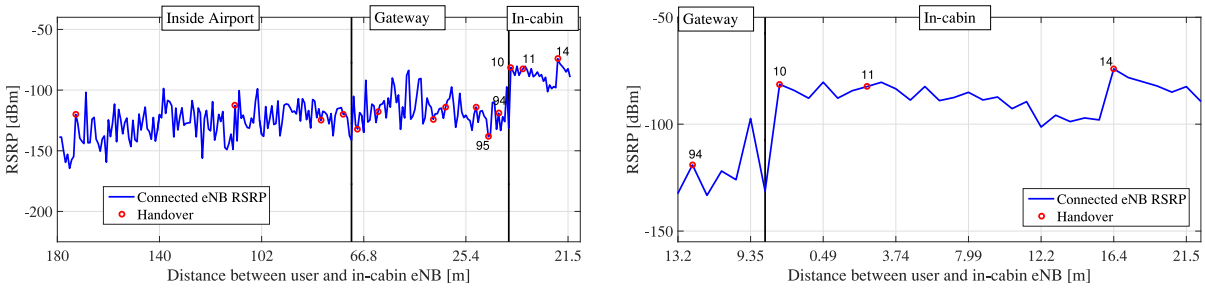

(a) Full Scale (b) In-Cabin

Fig. 13. Handover occurrence for the moving user. Written number on the red circles represents serving eNB after handover - eNB index equal or smaller than 24 represents in-cabin eNBs (there are 3 aircraft, in each aircraft there are 2 eNBs and in each eNB there are 4 cells) and larger than 24 represents terrestrial eNBs. (a) Full Scale. (b) In-Cabin.

TABLE IV
EVENT A3 PARAMETERS

Parameter	Range	Unit	Notes
cellIndividualOffset	-24, -22,...,-2, -1, 0, 1, 2,...,22, 24	dB	Set as Q-OffsetRange
a3-Offset	-30,...,30	-	0.5×*a3-Offset* dB
Hysteresis	0,...,30	-	0.5×*Hysteresis* dB
TimeToTrigger	0, 40, 64, 80, 100, 128, 160, 256, 320, 480, 512, 640, 1024, 1280, 2560, 5120	ms	

TABLE V
DISTANCE BETWEEN THE TERRESTRIAL ENB AND AIRCRAFT FOR A GIVEN RSRP LEVEL

Desired RSRP Level	Distance
−50 dBm	50 m
−70 dBm	135 m
−90 dBm	500 m

in-cabin systems, −50 dBm, −70 dBm and −90 dBm of RSRP levels are considered outside the aircraft irrespective of the location of the eNBs. In Table V, an approximated distance between the terrestrial eNB and the aircraft is given for the noted RSRP levels when the transmission power and transmit antenna gain of the terrestrial eNB are set to 49 dBm and 16 dBi, respectively.

Based on the given handover parameters and RSRP levels from a terrestrial and in-cabin eNBs, the handover triggering threshold can be written as:

$$\text{RSRP}_{\text{out}} + \text{a3-Offset} + \text{hysteresis} < \text{RSRP}_{\text{in}} + \text{CIO}, \quad (13)$$

where RSRP_{out} is the RSRP level from a terrestrial eNB; RSRP_{in} is the highest RSRP level in front of the aircraft entrance door when a user onboard the aircraft; and CIO represents *cellIndividualOffset*. The possible *cellIndividualOffset* values can be obtained based on the achieved RSRP_{out}, RSRP_{in} and the used handover parameters, namely *a3-Offset* and *hysteresis*[9]. For example, lets consider that RSRP_{out}, *a3-Offset* and *hysteresis* are equal to −90 dBm, 10 dB and 5 dB, respectively. When the in-cabin eNB transmission power is set to 10.2 dBm, RSRP_{in} is −78.9 dBm around the aircraft front entrance door. Accordingly, for the given example, the *cellIndividualOffset* should be set to 4 dB to satisfy (13) to handover the user as soon as boards the aircraft. However, for the given example, if the considered RSRP_{out} level is equal to −50 dBm, then there is no *cellIndividualOffset* value in its prescribed range – the maximum value of the *cellIndividualOffset* is 24 dB. Therefore, for such a case, the *a3-offset* and *hysteresis* parameters of the terrestrial eNB should be set to lower values, as depicted in Fig. 4.

[9]Range of *a3-Offset*, *hysteresis* and *cellIndividualOffset* parameters can be found in Table IV.

VIII. CONCLUSION

In this study, compatibility between an in-cabin LTE system and the existing terrestrial LTE network is investigated while the aircraft is parked on the airport apron which is structured based on the linear apron concept. Although the ECC reports and decisions state that an in-cabin mobile communication system should not be activated/operated while the aircraft is on the ground or during take-off and landing (only active when the altitude of the aircraft is above 3000 m), it is of interest to establish the effects such operation would have on the existing terrestrial networks. Accordingly, Edinburgh Airport and existing LTE eNBs covering the airport are modeled in this study. Generally accepted and validated WINNER channel models are used to model link between terrestrial eNBs and all classes of users, and a channel model obtained from in-cabin measurement campaign data is used to model channel between the in-cabin eNBs and in-cabin users.

Based on interference power performance results of the systems with and without in-cabin LTE eNBs, an in-cabin LTE system can be operated within the existing LTE network without causing almost any interference. There should be an exception for the users who are in the process of boarding the aircraft by use of a passenger bridge. To mitigate possible harmful interference to the existing LTE network users on the passenger bridge, the in-cabin LTE system could be operated only after boarding is completed and the passenger bridge is empty.

In addition, users who are connected to the terrestrial network are split between the different operators and only allowed to connect to their operator's eNBs. The process through which

UE attaches to an eNB is also studied in detail, in order to understand if there are any other challenges associated with having a limitation on the number of users that an eNB can serve. Based on the SINR performance results with and without in-cabin LTE eNBs, when a user cannot connect to an eNB that serves the best average received power, the performance degradation due to the presence of the in-cabin eNBs is negligible.

In conclusion, it is shown that the in-cabin LTE network does not interact significantly with the terrestrial LTE network and vice versa in the downlink direction. This means that there should not be any significant challenges from a signal quality and network management perspective that need to be solved in order for the two networks to co-exist. Therefore, it is essential that the legislation that prohibits the use of mobile devices onboard aircraft is reviewed, so that the necessary steps can be taken to enter the next generation of communication systems, which will provide seamless mobile connectivity.

REFERENCES

[1] D. B. Walen, R. A. Chitwood, B. DeCleene, and T. Shave, "Study on the user of cell phones on passenger aircraft," Federal Aviation Admin., Washington, DC, USA, Tech. Rep. DOT/FAA/AR-12/30, Jul. 2012.

[2] FCC, "Expanding access to mobile wireless services onboard aircraft notice of proposed rulemaking," Federal Commun. Commission, Washington, DC, USA, Tech. Rep. FCC 13-157, Dec. 2013.

[3] FCC, "Expanding access to broadband and encouraging innovation through establishment of an air-ground mobile broadband secondary service for passengers aboard aircraft in the 14.0-14.5 GHz band notice of proposed rulemaking," Federal Commun. Commission, Washington, DC, USA, Tech. Rep. FCC 13-66, May 2013.

[4] ECC, "The harmonised use of airborne GSM and LTE systems in the frequency bands 1710–1785 MHz and 1805–1880 MHz, and airborne UMTS systems in the frequency bands 1920–1980 MHz and 2110–2170 MHz (Amended 14 March 2014)," Electronic Commun. Committee, Copenhagen, Denmark, ECC Decision (06)07, 2006.

[5] ECC, "Compatibility between GSM equipment on board aircraft and terrestrial networks (Revised May 2008)," Electronic Commun. Committee, Copenhagen, Denmark, ECC Rep. 93, 2006.

[6] ECC, "On harmonised conditions of spectrum use for the operation of mobile communication services on aircraft (MCA Services) in the community," Electronic Commun. Committee, Copenhagen, Denmark, ECC Decision 2008/294/EC, 2008.

[7] ECC, "Compatibility study between mobile communication services on board aircraft (MCA) and ground-based systems," Electronic Commun. Committee, Copenhagen, Denmark, ECC Rep. 187, 2013.

[8] ECC, "Amending decision 2008/294/EC to include additional access technologies and frequency bands for mobile communication services on aircraft (MCA services)," Electron. Commun. Committee, Copenhagen, Denmark, ECC Decis. 2013/654/EU, 2013.

[9] E. Dinc *et al.*, "In-flight broadband connectivity: Architectures and business models for high capacity air-to-ground communications," *IEEE Commun. Mag.*, vol. 55, no. 9, pp. 142–149, Aug. 2017.

[10] ECC, "Broadband direct-air-to-ground communications (DA2GC)," Electron. Commun. Committee, Copenhagen, Denmark, ECC Rep. 214, May 2014.

[11] T. Cogalan, S. Videv, and H. Haas, "Performance optimization of aircraft in-cabin LTE deployment using Taguchi's method," in *Proc. IEEE Int. Conf. Commun.*, Jun. 2015, pp. 3125–3130.

[12] N. Moraitis, P. Constantinou, F. Perez-Fontan, and P. Valtr, "Propagation measurements and comparison with EM techniques for in-cabin wireless networks," *EURASIP J. Wireless Commun. Netw.*, vol. 2009, 2009, Art. no. 5.

[13] *Further Advancements for E-UTRA Physical Layer Aspects (Release 9)*, 3GPP TR 36.814 V9.0.0 (2010-03), Sep. 3, 2010. [Online]. Available: www.3gpp.org/ftp/Specs/. Accessed on: Sep. 3, 2010.

[14] [Online]. Available: http://www.edinburghairport.com/about-us/facts-and-figures, Accessed on: Feb. 2018.

[15] ICAO, "Airport planning manual," Int. Civil Aviation Org., Montreal, QC, Canada, Doc. 9184-AN/902 Part 1, 1987.

[16] OFCOM, "Licences of UK cellular operators," Jan. 2015. [Online]. Available: http://licensing.ofcom.org.uk/radiocommunication-licences/mobile-wireless-broadband/cellular-wireless-broadband/policy-and-background/licensee-freq-tech-information/uk-cellular-operators/

[17] P. Kyosti *et al.*, "WINNER II channel models," Inf. Soc. Technol., Yerevan, Armenia, Tech. Rep. D1.1.2 V1.2, WINNER, 2008.

[18] J. Meinila *et al.*, "WINNER+ final channel models," Celtic Telecommun. Solutions, Heidelberg, Germany, Tech. Rep. D5.3, WINNER+, 2010.

[19] *LTE; Evolved Universal Terrestrial Radio Access (E-UTRA); Physical Layer; Measurements (Release 13)*," 3GPP TS 36.214 V13.0.0, Jan. 2016.

[20] *LTE; Evolved Universal Terrestrial Radio Access (E-UTRA); Physical Channels and Modulation (Release 13)*, 3GPP TS 36.211 V13.0.0, Jan. 2016.

[21] OFCOM, "Variation of 1800 MHz mobile licences to increase power limit," Statement, Aug. 2014.

Tezcan Cogalan (S'10) received the B.Sc. and M.Sc. degrees from Kadir Has University, Istanbul, Turkey, in 2011 and 2013, respectively. He is currently working toward the Ph.D. degree with the Institute for Digital Communications, Li-Fi R&D Center, The University of Edinburgh, Edinburgh, U.K. His research interests include interference analysis, radio resource management and optimization of wireless communication systems for user dense environments.

Stefan Videv received the B.Sc. degree in electrical engineering and computer science and the M.Sc. degree in communications, systems and electronics from Jacobs University, Bremen, Germany, in 2007 and 2009, respectively, and the Ph.D. degree from The University of Edinburgh, Edinburgh, U.K., in 2013, for the thesis titled "Techniques for Green Radio Cellular Communications." He is currently the Director Engineering with the Li-Fi R&D Center, The University of Edinburgh, working in the field of visible light communications. His research focuses on quick prototyping of communication systems, smart resource allocation, and energy efficient communications.

Harald Haas (S'98–AM'00–M'03–SM'16–F'17) received the Ph.D. degree from The University of Edinburgh, Edinburgh, U.K., in 2001. He is currently the Chair of mobile communications with The University of Edinburgh, and is the Initiator, Co-Founder, and Chief Scientific Officer of pureLiFi, Ltd., Edinburgh, U.K., and the Director of the LiFi Research and Development Centre, The University of Edinburgh. He has authored 430 conference and journal papers, including a paper in Science and coauthored a book *Principles of LED Light Communications: Towards Networked Li-Fi* (Cambridge Univ. Press, 2015). His main research interests include optical wireless communications, hybrid optical wireless and RF communications, spatial modulation, and interference coordination in wireless networks. He first introduced and coined spatial modulation and LiFi. LiFi was listed among the 50 best inventions in TIME Magazine in 2011. He was an invited speaker at TED Global 2011, and his talk on Wireless Data from Every Light Bulb has been watched online over 2.4 million times. He gave a second TED Global lecture in 2015 on the use of solar cells as LiFi data detectors and energy harvesters. This has been viewed online over 2 million times. He was elected as a Fellow of the Royal Society of Edinburghin 2017. In 2012 and 2017, he was a recipient of the prestigious Established Career Fellowship from the Engineering and Physical Sciences Research Council, Information and Communications Technology, U.K. In 2014, he was selected by EPSRC as one of ten Recognizing Inspirational Scientists and Engineers Leaders in the U.K. He was a corecipient of the EURASIP Best Paper Award for the *Journal on Wireless Communications and Networking* in 2015 and the Jack Neubauer Memorial Award of the IEEE Vehicular Technology Society. In 2016, he was the recipient of the Outstanding Achievement Award from the International Solid State Lighting Alliance. He was a corecipient of recent best paper awards at VTC-Fall, 2013, VTC-Spring 2015, ICC 2016, ICC 2017, and ICC 2018. He is an Editor of the IEEE TRANSACTIONS ON COMMUNICATIONS and the IEEE JOURNAL OF LIGHTWAVE TECHNOLOGIES.